Full Paper
doi.org/10.1002/chem.202001510

Coordination Chemistry |Hot Paper|

Multinuclear Pt^{II} Complexes: Why Three is Better Than Two to Enhance Photophysical Properties

Sourav Chakraborty,[a] Alessandro Aliprandi,[a] and Luisa De Cola*[a, b]

Abstract: The self-assembly of platinum complexes is a well-documented process that leads to interesting changes of the photophysical and electrochemical behavior as well as to a change in reactivity of the complexes. However, it is still not clear how many metal units must interact in order to achieve the desired properties of a large assembly. This work aimed to clarify the role of the number of interacting Pt^{II} units leading to an enhancement of the spectroscopic properties and how to address inter- versus intramolecular processes. Therefore, a series of neutral multinuclear Pt^{II} complexes were synthesized and characterized, and their photophysical properties at different concentration were studied. Going from the monomer to dimers, the growth of a new emission band and the enhancement of the emission properties were observed. Upon increasing the platinum units up to three, the monomeric blue emission could not be detected anymore and a concentration independent bright-yellow/orange emission, due to the establishment of intramolecular metallophilic interactions, was observed.

Introduction

Square planar Pt^{II} complexes containing conjugated coordinated ligands are particularly interesting building blocks for the creation of supramolecular nanostructures since their flat geometry makes them prone to stack through noncovalent interaction, such as π–π stacking.[1–10] Furthermore, when Pt^{II} complexes are close enough (distance below 3.5 Å)[11–14] metallophilic interactions between Pt centers may be established and stable aggregates[15–17] can be observed that possess spectroscopic properties which can be dramatically different from those of the monomeric metal complex.[1–4,18–23] In fact, the establishment of ground state intermolecular interactions between protruding d_{z^2} orbitals results in the formation of lower-lying molecular orbitals, thus a new optical transition appears ascribed to metal–metal-to-ligand charge transfer (MMLCT).[22–28] The changes in the optical properties are directly correlated with the distance between the Pt centers.[6,11,29–31] Thus, the shorter the distance is, the stronger the electronic Pt···Pt electronic interaction is, and the more bathochromically shifted the MMLCT band is.[32–33] However, the formation of assembled species not only changes the absorption and emission energy, but also leads often to an enhancement of the emission quantum yields (PLQY) and to an elongation of the excited state lifetime, due to a change of the nature of the lowest transition and the increasing rigidity of the packed units.[20] Our group has recently reported a phosphorescent mononuclear amphiphilic Pt^{II}-complex[20] (PLQY of 1% in aerated dioxane) capable of producing strong orange phosphorescence with a PLQY up to 84% in water/dioxane (95:5) solution. The very high PLQY in aerated solution suggests also a protection of the packed Pt^{II} centers from dioxygen. Indeed, due to the triplet nature of the platinum complexes emissions, one would expect strong quenching, by dioxygen, of the long lived (microsecond) excited state. The outstanding photophysical properties of self-assembled structures of Pt^{II} complexes have gained high popularity in the last decades due to their good performances in several applications, such as organic light-emitting diodes (OLEDs),[18,34–39] field effect transistors (FETs),[40,41] organic light-emitting FETs (OLEFETs)[42] and, more recently, as sensors[43–49] and as labels in electrochemiluminescent systems.[20,50] However the self-assembly of such compounds requires not only a precise chemical design, but also a tight control of several parameters, such as solvent composition, temperature and pH.

An interesting open question is how many units are needed to obtained a full change in the spectroscopic behavior, as

[a] Dr. S. Chakraborty, Dr. A. Aliprandi, Prof. L. De Cola
Institut de Science et d'Ingénierie Supramoléculaires
CNRS, UMR 7006, Université de Strasbourg
8 rue Gaspard Monge, 67000 Strasbourg (France)
E-mail: decola@unistra.fr

[b] Prof. L. De Cola
Institute for Nanotechnology (INT)
Karlsruhe Institute of Technology
Hermann-von-Helmholtz-Platz 1
76344 Eggenstein-Leopoldshafen (Germany)

Supporting information and the ORCID identification number(s) for the author(s) of this article can be found under: https://doi.org/10.1002/chem.202001510.

Part of a Special Issue for the 8th EuChemS Chemistry Congress consisting of contributions from selected speakers and conveners. To view the complete issue, visit Issue 48.

that observed for large assembled structures. A strategy to solve such a fundamental problem is to design multinuclear Pt^{II} complexes in which the establishment of Pt···Pt and/or π–π stacking interactions is obtained by polytopic auxiliary ligands.[51–53] For example, Che and co-workers[54] reported a series of trinuclear tridentate cyclometalated platinum(II) complexes, tethered by *tris*-phosphine auxiliary linkers, and compared the photophysical properties with those of their mono- and binuclear homologues. However, the behavior of the reported multinuclear Pt^{II}-complexes in solution has not been reported at different concentrations to unravel the intermolecular versus intramolecular interactions.

Despite several reported dinuclear complexes,[25,55–58] to the best of our knowledge, a clear answer to the above question has not been given yet. Indeed, all the reported cases show a change in the emission color when a Pt···Pt interaction is established, but how the enhancement of the emission properties is correlated to the number of units involved in the assemblies is still under debate.

Herein, we aim to answer these fundamental questions by comparing the spectroscopic properties of a series of neutral mono-, bis-, and tris-Pt^{II} complexes at different concentrations in order to assess intra versus intermolecular processes. The luminescent compounds consist of a tridentate dianionic 2,6-*bis*(1H-1,2,4-triazol-5-yl)pyridine[59] chelates and ancillary tetraethylene glycol-substituted pyridine ligands (Scheme 1). We have prepared two dimers in which the phenyl ring is substituted at the 1,2 and 1,3 positions to evaluate the effects of intermolecular versus intramolecular interactions on the photophysical properties.

The rationalization of the photophysical behavior observed for the different species at different concentrations in solution allows for the design of molecularly defined systems possessing high phosphorescence quantum yields and long excited state lifetimes even in aerated solvents.

Results and Discussion

Synthesis and characterization

The multinuclear complexes were prepared by attaching the pyridines substituted at position 4 with a tetraethylene glycol (TEG) chain to di- and trihydroxy benzene, and then by reacting the pyridines with a platinum precursor. In particular, the mono-pyridine linker **L1** (see Supporting Information, Scheme S1) was functionalized by heating to reflux a stirred CH_3CN solution of tetraethylene glycol monomethyl ether with 4-(chloromethyl)-pyridine hydrochloride in the presence of NaH under nitrogen.[60] Whereas, the synthesis of bis-pyridine (**L2 a**, and **L2 b**) and tris-pyridine (**L3**) linkers were achieved in two steps. First, the condensation of the monotosylated tetraethylene glycol with appropriate di- and tri-hydroxy benzene resulted in the formation of the corresponding di- and tri-TEG precursors (see Supporting Information, Schemes S2–S4). These di- and tri-TEG precursors were subsequently treated with 4-(chloromethyl)pyridine hydrochloride in the presence of sodium hydride under nitrogen to generate the expected TEG functionalized 1,3-bispyridine (**L2 a**), 1,2-bispyridine (**L2 b**), and 1,2,3-trispyridine (**L3**) linkers in good to moderate yields (see Supporting Information, Schemes S2–S4). The ^{1}H NMR spectra of the linkers (**L1-L3**) shows a distinctive sharp singlet, at $\delta =$ 4.61, 4.51, 4.58 and 4.62 ppm, respectively, due to the benzylic -O*C*H_2 linkage, two doublets for the pyridine protons in the aromatic region and the characteristic signals for glycol chains between 3.5 and 4.3 ppm suggest the formation of the anticipated pyridine linkers which was further supported by ESI-MS data (see Supporting Information for detailed characterization).

In order to synthesize the desired Pt^{II} complexes, Pyridine linkers **L1-L4** were treated with $PtCl_2(DMSO)_2$ as the platinum precursor, 2,6-bis[3-(trifluoromethyl)-1*H*-1,2,4-triazol-5-yl] pyridine[59] as the tridentate auxiliary ligand (py-CF3-trzH_2) in $CHCl_3$, and in the presence of Hünig base (*i*Pr_2EtN) at 50 °C to obtain the corresponding *mono*Pt(II), **Pt1**, 1,3-*bis*Pt(II) **Pt2 a**, 1,2- *bis*Pt(II), **Pt2 b**, and 1,2,3-*tris*Pt(II), **Pt3**, complexes (Scheme 1). The ^{1}H NMR spectra of **Pt1**, **Pt2 a** and **Pt2 b** complexes (Figures S4, S14, S23) show a large downfield shift of

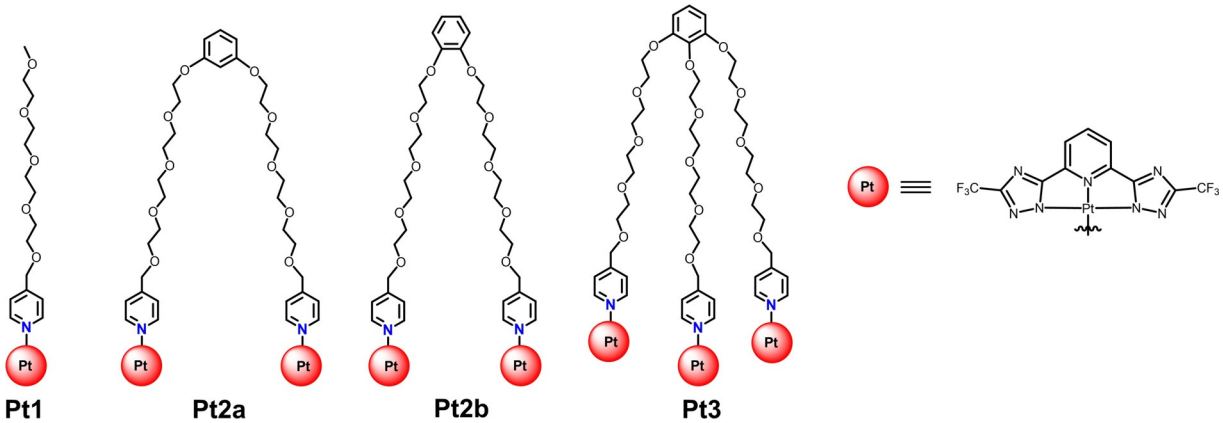

Scheme 1. Chemical formulas of monoPt(II) **Pt1**, 1,3-bisPt(II), **Pt2 a**, 1,2-bisPt(II), **Pt2 b**, and 1,2,3-trisPt(II), **Pt3** complexes.

pyridine protons adjacent to the nitrogen donor atom, confirming the metal-ligand coordination. The other pyridine protons, as well as the protons from auxiliary tridentate linkers, also shifts downfield compared to their non-complexed analogues. The appearance of a sharp singlet in the ^{19}F NMR spectra of complexes **Pt1**, **Pt2a** and **Pt2b** at $\delta = -64.2$, -64.5 and -64.4 ppm, respectively, suggests the overall symmetry of these complexes (Figures S6, S15, S24). However, in the case of complex **Pt3** two peaks (-64.09 and -64.10) were observed in the ^{19}F NMR spectrum (Figure S32), suggesting the presence of two different chemical environments for the three platinum complex units. In the ^{1}H NMR (Figure S33) spectrum, the appearance of two sets of aromatic peaks, for the **Pt3**, in 1:2 ratio further confirms that we have a trimetallic system in which the central platinum feels a different chemical environment than the external platinum units. The chemical characterization was completed by high-resolution mass spectrometry analysis (see Supporting Information). All mass peaks are isotopically resolved and in good agreement with the theoretically predicted isotopic distribution, further confirming the formation of desired complexes.

Photophysical characterization

Complexes **Pt1–Pt3** were fully characterized by using electronic absorption, steady-state and time-resolved emission spectroscopy at different concentrations, from 1 to 100 μM in CH_2Cl_2 (DCM). As shown in Figure 1a, the absorption spectra of **Pt1** display intense bands in the UV region ($\lambda = 254$ nm, 300 nm, 337 nm). These transitions are mainly attributed to intra-ligand (^{1}IL) and metal-perturbed inter-ligand charge transfer (^{1}ILCT) states. At lower energy, in the 360–450 nm range, broad and featureless weak bands with molar extinction coefficients, ε, between 0.99 and 4.3×10^3 M^{-1}cm^{-1} (calculated at $\lambda_{abs} = 402$ nm) for all the complexes were assigned to transitions involving the spin-allowed singlet-manifold metal-to-ligand charge transfer, ^{1}MLCT, and the forbidden singlet to triplet, ^{3}MLCT, partially allowed due to the presence of the heavy atom. These excitation processes have been previously reported for similar cyclometalated platinum(II) complexes.[37] Increasing the concentration from 1 μM to 100 μM did not lead to a change in the features of the absorption spectra, suggesting that **Pt1** exist in the monomeric form in such range of concentrations. The absence of concentration-dependent aggregation is also evident in the emission spectra that are all characterized by a moderate structured emission (PLQY = 1.5%) in the blue region of the visible spectrum with maximum at 463 nm, and vibrational bands at 491, 525, and a shoulder at 570 nm (Figure 1b). Also the excited state lifetimes seems to be unaffected by the concentration, with an average value of 188 ns in aerated DCM (see Table 1 for details). The steady state luminescence as well as the excited-state lifetime of the complex are typical of the monomeric form of this class of compounds.[19–20, 29, 50, 60, 61]

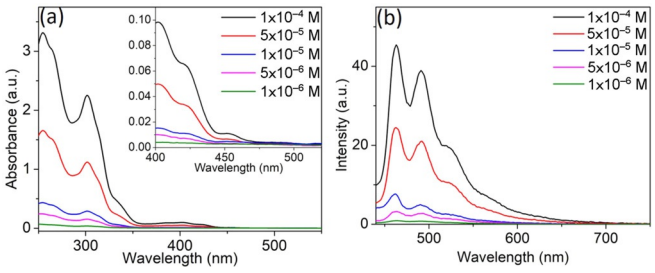

Figure 1. (a) UV/Vis absorption spectra and (b) emission spectra, $\lambda_{exc} = 375$ nm, for complex **Pt1** at variable concentration (1 μM to 100 μM) in DCM.

Table 1. Photophysical data of platinum complexes **Pt1–Pt3** in DCM (5×10^{-5} M) at room temperature.

Complex	λ_{abs} [nm] (ε [10^3 M^{-1} cm^{-1}])	λ_{ex} [nm]	$\lambda_{em,max}$ nm	Lifetime (τ) [ns]	Φ_{PL}
Pt1	254 (33.2) 300 (22.2) 337 (3.9) 402 (0.99)	375	460 485 525	$\tau_1 = 188.2$ (88%) $\tau_2 = 3.8$ (12%)	0.015
Pt2a	254 (66.4) 300 (38) 337 (8.3) 402 (2.4)	375	580 460 	$\tau_1 = 1013.6$ (88%) $\tau_2 = 14.4$ (12%) $\tau_1 = 258.1$ (88%) $\tau_2 = 11.7$ (12%)	0.029
Pt2b	254 (56) 300 (32) 337 (7.2) 402 (2.1)	375	580 460 	$\tau_1 = 1029.0$ (66%) $\tau_2 = 21.8$ (34%) $\tau_1 = 235.8$ (38%) $\tau_2 = 14.5$ (62%)	0.027
Pt3	256 (69.6) 300 (36.6) 337 (9.8) 402(4.3)	400	590	$\tau = 1093.1$	0.38

Both **Pt2a** and **Pt2b** complexes show the aggregate intense emission band at around 580 nm along with the peaks in blue region, which shows slight shifts featuring emission maxima at 466 and 494 mm for **Pt2a** and 468 and 497 mm for complex **Pt2b** (PLQY = 2.9% and 2.7% for **Pt2a** and **Pt2b**, respectively at 5×10^{-6} M). The absorption spectra suggest that the aggregation is already in the ground state as clearly seen (Figure 2a,b) compared with the reference compound **Pt1** in which the band in the visible region is much less pronounced than for **Pt2a** and **Pt2b**. This is true even though working at the same molar concentration means that for the dimer we have twice the number of platinum units than for the monomer and therefore a double absorbance, in the absence of other factors. Such data are confirmed by the excitation spectra of both the complexes at $\lambda_{em} = 580$ nm, clearly displaying a lower energy excitation band that trace up to 500 nm (see Supporting Information, Figures S37 and S40) which is ascribed to ^{3}MMLCT transitions due to the establishment of Pt···Pt metallophilic interactions.

As expected at high concentration both **Pt2a** and **Pt2b** (Figure 2a,c) show a great tendency to form intermolecular interactions rather than only intramolecular ones. However, a careful examination of the emission spectra upon excitation at

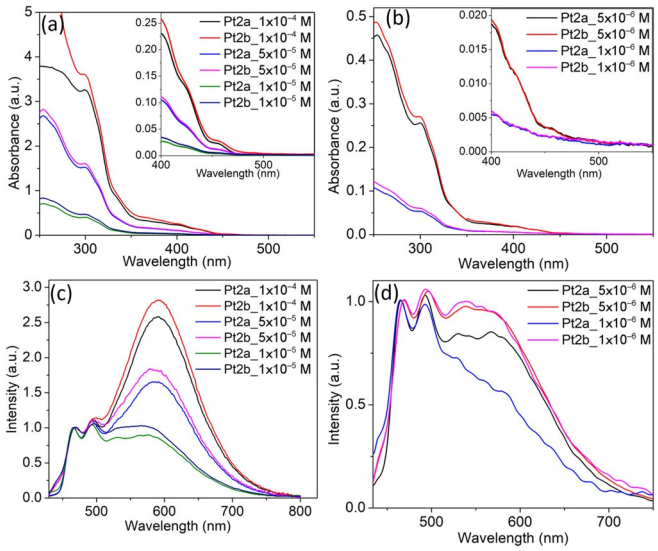

Figure 2. (a, b) UV/Vis absorption spectra and (c, d) normalized (at 467 nm) Emission spectra (upon $\lambda_{exc}=375$ nm) for complex **Pt2a** and **Pt2b** at variable concentration (100 μM to 1 μM) in DCM.

375 nm in DCM solutions reveals that the two compounds behave differently at low concentration. In fact, the relative emission intensities of the monomeric band (467 nm) versus the aggregate band (580 nm) is not the same for the two systems, as one would predict from their chemical structure. For **Pt2a**, the distance between the two complexes, despite the flexibility of the glycol chains, is definitely larger than for **Pt2b** and indeed at 1×10^{-6} M and at 5×10^{-6} M solutions the ratio between the high and low energy bands (467 vs. 580 nm) is much higher for complex **Pt2a** than for **Pt2b** (Figure 2d). Such behavior can be rationalized assuming that at such concentrations the predominant interactions are intramolecular and therefore the capability to establish intramolecular metallophilic interactions is higher for **Pt2b** than for **Pt2a**. Increasing the concentration leads to a large increase of the emission intensity at 580 nm compared to the band at 467 nm, suggesting the establishment of intermolecular interactions. Not surprisingly, in this range of concentrations both dimers behave similarly (Figure 2c). A possible mechanism is depicted in Scheme 2 according to which, while **Pt1** is more stable in the solvated monomeric form, the dimers are more prone to intercalation with other molecules. The corresponding excited state lifetimes of the bands at 460 nm and 580 nm of **Pt2a** and **Pt2b** at different concentrations are shown in Tables S2 and S3 in the Supporting Information, respectively. The longer lifetime component, attributed to ^{3}MMLCT decay, increases its relative weight at higher concentration (see Supporting Information Table S2 and S3). Noticeably, for both complexes on decreasing the concentration from 100 to 1 μM the lifetime of the long component attributed to the ^{3}MMLCT transition decreases gradually from 1 to 0.7 μs suggesting an effective dioxygen quenching when the intramolecular interactions are reduced. Indeed the excited state lifetimes recorded in deaerated 1 μM solutions for both complex **Pt2a** and **Pt2b** are close to the one recorded for aerated high concentrated (100 μM) solutions, as shown in Table 2.

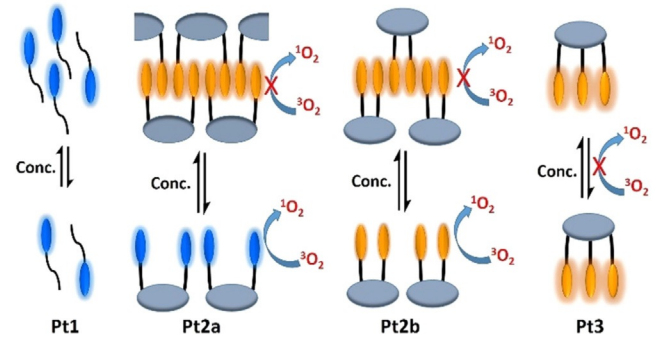

Scheme 2. Mechanistic illustration of the intra and intermolecular aggregation of the Pt(II) complexes from high concentration (on top) to diluted solutions (bottom).

Table 2. Excited state lifetimes (τ) of **Pt2a**, **Pt2b**, and **Pt3** at different concentrations with and without oxygen recorded at $\lambda_{em}=580$ nm, by using $\lambda_{exc}=375$ nm.

Concentration [M]	**Pt2a** τ [ns]	**Pt2b** τ [ns]	**Pt3** τ [ns]
1×10^{-4}	$\tau_1=1058.1$ (94%) $\tau_2=15.4$ (6%)	$\tau_1=1072.4$ (76%) $\tau_2=22.9$ (24%)	1084.7
5×10^{-5}	$\tau_1=1013.6$ (88%) $\tau_2=14.6$ (12%)	$\tau_1=1029.0$ (66%) $\tau_2=21.8$ (34%)	1093.1
1×10^{-5}	$\tau_1=851.6$ (75%) $\tau_2=13.5$ (25%)	$\tau_1=855.4$ (52%) $\tau_2=23.9$ (48%)	1122.6
5×10^{-6}	$\tau_1=782.7$ (71%) $\tau_2=13.2$ (28%)	$\tau_1=796.2$ (33%) $\tau_2=20.7$ (67%)	1126.7
1×10^{-6}	$\tau_1=702.9$ (62%) $\tau_2=12.8$ ns (38%)	$\tau_1=708.4$ (44%) $\tau_2=22.0$ (56%)	1222.5
1×10^{-6} deaerated	$\tau_1=1107.1$ (66%) $\tau_2=12.6$ (34%)	$\tau_1=902.1$ (53%) $\tau_2=24.3$ (47%)	1480.4

Interestingly, by increasing the number of Pt^{II} units from two to three the scenario changes completely as shown in Figure 3. Complex **Pt3** displays a more intense low-energy absorption band centered at about 461 nm and stretching towards 500 nm (Figure 3a, inset). We can definitely state that the bands at lowest energy are metal–metal-to-ligand charge transfer (^{1}MMLCT and ^{3}MMLCT) transitions[12,62] associated to the formation of Pt···Pt and π–π stacking interactions. In the case of **Pt3** the MMLCT bands are independent from the concentration and are present even in very dilute conditions suggesting strong intramolecular electronic interactions. Upon excitation at 400 nm, **Pt3** shows only one very intense emission band centered at 590 nm (Figure 3) with a PLQY value up to 38% in air-equilibrated DCM solutions. The excited state decays with a mono-exponential kinetic of around 1 μs (see Table S4), which is ascribed to a ^{3}MMLCT transition resulting

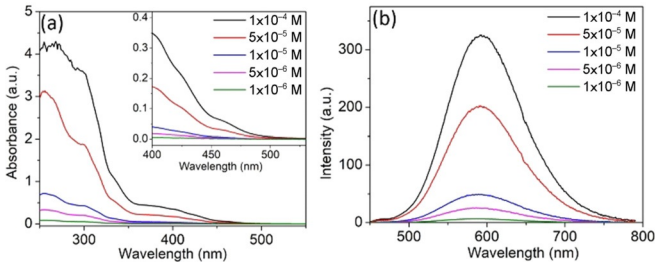

Figure 3. (a) UV/Vis absorption spectra, and (b) emission spectra (upon $\lambda_{exc} = 400$ nm) for complex **Pt3** at different concentrations (0.1 mM to 1.0 μM) in DCM.

from intramolecular metallophilic interactions. The ground state interaction between platinum units is also confirmed by the appearance of the typical MMLCT bands stretching up to 500 nm in the excitation spectra of complex **Pt3**, monitored at the emission maximum (Figure S43). The concentration dependency of the emission spectra in range of 100 to 1 μM shows no effect on the emission profile of complex (Figure 3 b) as well as the lifetime decay of the excited state component remains unchanged (see Table 2). In addition, for such complex the elimination of the dioxygen from the solution does not have any pronounced effect on the exited state lifetime, which showed only a marginal elongation (Scheme 2).

We can therefore conclude that for **Pt3** the ^{3}MMLCT emitting state is tightly packed, as shown by the high emission quantum yield and by the lack of diffusion of the dioxygen that should quench such long-lived emitters.

Conclusions

To rationalize the properties emerging from the self-assembly of luminescent platinum complexes, and in particular the role played by the number of units to reach the enhancement of the photophysical properties, we have investigated a series of neutral mono-, bis- and tris-platinum(II) complexes. The compounds are based on platinum metal ions, a tridentate N^N^N chromophoric auxiliary ligand and TEG-functionalized mono-, di- or tri-pyridine linkers. The complex possessing a single Pt center, **Pt1**, is characterized by a blue emission and showed no intermolecular Pt···Pt interactions in a large range of concentration (1–100 μM). Going from monomer to dimers leads to concentration-dependent luminescence in which both monomeric and aggregate emissions are observed. Increasing further the number of Pt complexes to three results in the complete disappearance of blue emission and an orange phosphorescence which is unaffected by concentration. We concluded that even though dimeric species can already cause the shift in the emission properties, due to the rising of the MMLCT emission, we need at least three units to fully benefit of the assembly emerging properties, with the elongation of the excited state lifetime, protection from the dioxygen quenching and increase in the emission quantum yields.

Acknowledgements

S.C., A.A., and L.D.C. kindly acknowledge the University of Strasbourg, and the CNRS for financial support. L.D.C. is grateful to AXA Research funding and Institut Universitaire de France (IUF) for financial support.

Conflict of interest

The authors declare no conflict of interest.

Keywords: aggregation-induced emission · luminescence · metallophilic interactions · multinuclear · platinum

[1] P. Pyykkö, *Chem. Rev.* **1997**, *97*, 597–636.
[2] M. Mauro, A. Aliprandi, D. Septiadi, N. S. Kehr, L. De Cola, *Chem. Soc. Rev.* **2014**, *43*, 4144–4166.
[3] V. W. Yam, V. K. Au, S. Y. Leung, *Chem. Rev.* **2015**, *115*, 7589–7728.
[4] A. Aliprandi, D. Genovese, M. Mauro, L. De Cola, *Chem. Lett.* **2015**, *44*, 1152–1169.
[5] K. Li, G. S. Ming Tong, Q. Wan, G. Cheng, W.-Y. Tong, W.-H. Ang, W.-L. Kwong, C.-M. Che, *Chem. Sci.* **2016**, *7*, 1653–1673.
[6] M. Krikorian, S. Liu, T. M. Swager, *J. Am. Chem. Soc.* **2014**, *136*, 2952–2955.
[7] M. E. Robinson, A. Nazemi, D. J. Lunn, D. W. Hayward, C. E. Boott, M.-S. Hsiao, R. L. Harniman, S. A. Davis, G. R. Whittell, R. M. Richardson, L. De Cola, I. Manners, *ACS Nano* **2017**, *11*, 9162–9175.
[8] V. N. Kozhevnikov, B. Donnio, D. W. Bruce, *Angew. Chem. Int. Ed.* **2008**, *47*, 6286–6289; *Angew. Chem.* **2008**, *120*, 6382–6385.
[9] K. Y. Kim, J. Kim, C. J. Moon, J. Liu, S. S. Lee, M. Y. Choi, C. Feng, J. H. Jung, *Angew. Chem. Int. Ed.* **2019**, *58*, 11709–11714; *Angew. Chem.* **2019**, *131*, 11835–11840.
[10] J. Zhao, Z. Feng, D. Zhong, X. Yang, Y. Wu, G. Zhou, Z. Wu, *Chem. Mater.* **2018**, *30*, 929–946.
[11] B. Ma, J. Li, P. I. Djurovich, M. Yousufuddin, R. Bau, M. E. Thompson, *J. Am. Chem. Soc.* **2005**, *127*, 28–29.
[12] C. A. Strassert, M. Mauro, L. De Cola, in *Advances in Inorganic Chemistry Vol. 63* (Eds.: R. van Eldik, G. Stochel), Elsevier Academic Press, San Diego, **2011**, pp. 47–103.
[13] D. Kim, J.-L. Brédas, *J. Am. Chem. Soc.* **2009**, *131*, 11371–11380.
[14] V. M. Miskowski, V. H. Houlding, *Inorg. Chem.* **1991**, *30*, 4446–4452.
[15] A. F. Suleymanova, O. S. Eltsov, D. N. Kozhevnikov, A. O. Lantushenko, M. P. Evstigneev, V. N. Kozhevnikov, *ChemistrySelect* **2017**, *2*, 3353–3355.
[16] M. Yoshida, M. Kato, *Coord. Chem. Rev.* **2018**, *355*, 101–115.
[17] M. Z. Shafikov, R. Daniels, P. Pander, F. B. Dias, J. A. G. Williams, V. N. Kozhevnikov, *ACS Appl. Mater. Interfaces* **2019**, *11*, 8182–8193.
[18] C. A. Strassert, C. H. Chien, M. D. Galvez Lopez, D. Kourkoulos, D. Hertel, K. Meerholz, L. De Cola, *Angew. Chem. Int. Ed.* **2011**, *50*, 946–950; *Angew. Chem.* **2011**, *123*, 976–980.
[19] M. Mauro, A. Aliprandi, C. Cebrian, D. Wang, C. Kubel, L. De Cola, *Chem. Commun.* **2014**, *50*, 7269–7272.
[20] A. Aliprandi, M. Mauro, L. De Cola, *Nat. Chem.* **2016**, *8*, 10–15.
[21] H.-L. Au-Yeung, A. Y.-Y. Tam, S. Y.-L. Leung, V. W.-W. Yam, *Chem. Sci.* **2017**, *8*, 2267–2276.
[22] V. C. Wong, C. Po, S. Y. Leung, A. K. Chan, S. Yang, B. Zhu, X. Cui, V. W. Yam, *J. Am. Chem. Soc.* **2018**, *140*, 657–666.
[23] N. Liu, T. Lin, M. Wu, H.-K. Luo, S.-L. Huang, T. S. A. Hor, *J. Am. Chem. Soc.* **2019**, *141*, 9448–9452.
[24] M. E. Robinson, D. J. Lunn, A. Nazemi, G. R. Whittell, L. De Cola, I. Manners, *Chem. Commun.* **2015**, *51*, 15921–15924.
[25] M. H. Chan, S. Y. Leung, V. W. Yam, *J. Am. Chem. Soc.* **2019**, *141*, 12312–12321.
[26] Y. Wang, Y. Cai, L. Cao, M. Cen, Y. Chen, R. Zhang, T. Chen, H. Dai, L. Hu, Y. Yao, *Chem. Commun.* **2019**, *55*, 10132–10134.
[27] C.-Y. Sun, W.-P. To, F.-F. Hung, X.-L. Wang, Z.-M. Su, C.-M. Che, *Chem. Sci.* **2018**, *9*, 2357–2364.

[28] Y. Atoini, E. A. Prasetyanto, P. Chen, S. Silvestrini, J. Harrowfield, L. De Cola, *Chem. Eur. J.* **2018**, *24*, 12054 – 12060.
[29] S. Sinn, F. Biedermann, M. Vishe, A. Aliprandi, C. Besnard, J. Lacour, L. D. Cola, *ChemPhysChem* **2016**, *17*, 1829 – 1834.
[30] D. Genovese, A. Aliprandi, E. A. Prasetyanto, M. Mauro, M. Hirtz, H. Fuchs, Y. Fujita, H. Uji-I, S. Lebedkin, M. Kappes, L. De Cola, *Adv. Funct. Mater.* **2016**, *26*, 5271 – 5278.
[31] A. Aliprandi, C. M. Croisetu, M. Mauro, L. D. Cola, *Chem. Eur. J.* **2017**, *23*, 5957 – 5961.
[32] M. Yoshida, M. Kato, *Coord. Chem. Rev.* **2020**, *408*, 213194.
[33] Q. Wan, X. S. Xiao, W. P. To, W. Lu, Y. Chen, K. H. Low, C. M. Che, *Angew. Chem. Int. Ed.* **2018**, *57*, 17189 – 17193.
[34] C. Cebrián, M. Mauro, *Beilstein J. Org. Chem.* **2018**, *14*, 1459 – 1481.
[35] M.-C. Tang, A. K.-W. Chan, M.-Y. Chan, V. W.-W. Yam, *Top. Curr. Chem.* **2016**, *374*, 46.
[36] F. K. Kong, M. C. Tang, Y. C. Wong, M. Ng, M. Y. Chan, V. W. Yam, *J. Am. Chem. Soc.* **2017**, *139*, 6351 – 6362.
[37] C. Cebrián, M. Mauro, D. Kourkoulos, P. Mercandelli, D. Hertel, K. Meerholz, C. A. Strassert, L. De Cola, *Adv. Mater.* **2013**, *25*, 437 – 442.
[38] M. Taneda, T. Yasuki, C. Adachi, *Appl. Phys. Express* **2011**, *4*, 071602.
[39] M. A. Baldo, D. F. O'Brien, Y. You, A. Shoustikov, S. Sibley, M. E. Thompson, S. R. Forrest, *Nature* **1998**, *395*, 151 – 154.
[40] R. Wawrzinek, K. Muhieddine, M. Ullah, P. B. Koszo, P. E. Shaw, A. Grosjean, F. Maasoumi, D. M. Stoltzfus, J. K. Clegg, P. L. Burn, E. B. Namdas, S.-C. Lo, *Adv. Opt. Mater.* **2016**, *4*, 1867 – 1874.
[41] C.-M. Che, C.-F. Chow, M.-Y. Yuen, V. A. L. Roy, W. Lu, Y. Chen, S. S.-Y. Chui, N. Zhu, *Chem. Sci.* **2011**, *2*, 216 – 220.
[42] M.-Y. Yuen, V. A. L. Roy, W. Lu, S. C. F. Kui, G. S. M. Tong, M.-H. So, S. S.-Y. Chui, M. Muccini, J. Q. Ning, S. J. Xu, C.-M. Che, *Angew. Chem. Int. Ed.* **2008**, *47*, 9895 – 9899.
[43] A. S.-Y. Law, L. C.-C. Lee, M. C.-L. Yeung, K. K.-W. Lo, V. W.-W. Yam, *J. Am. Chem. Soc.* **2019**, *141*, 18570 – 18577.
[44] J. A. Thomas, *Dalton Trans.* **2011**, *40*, 12005 – 12016.
[45] E. Spain, S. Carrara, K. Adamson, H. Ma, R. O'Kennedy, L. De Cola, R. J. Forster, *ACS Omega* **2018**, *3*, 17116 – 17124.
[46] K. Zhang, M. C.-L. Yeung, S. Y.-L. Leung, V. W.-W. Yam, *ACS Appl. Mater. Interfaces* **2020**, *12*, 8503 – 8512.
[47] Y. Shigeta, A. Kobayashi, M. Yoshida, M. Kato, *Cryst. Growth Des.* **2018**, *18*, 3419 – 3427.
[48] K. Masako, *Bull. Chem. Soc. Jpn.* **2007**, *80*, 287 – 294.
[49] M. J. Bryant, J. M. Skelton, L. E. Hatcher, C. Stubbs, E. Madrid, A. R. Pallipurath, L. H. Thomas, C. H. Woodall, J. Christensen, S. Fuertes, T. P. Robinson, C. M. Beavers, S. J. Teat, M. R. Warren, F. Pradaux-Caggiano, A. Walsh, F. Marken, D. R. Carbery, S. C. Parker, N. B. McKeown, R. Malpass-Evans, M. Carta, P. R. Raithby, *Nat. Commun.* **2017**, *8*, 1800.
[50] S. Carrara, A. Aliprandi, C. F. Hogan, L. De Cola, *J. Am. Chem. Soc.* **2017**, *139*, 14605 – 14610.
[51] E. V. Puttock, M. T. Walden, J. A. G. Williams, *Coord. Chem. Rev.* **2018**, *367*, 127 – 162.
[52] W. Sun, H. Zhu, P. M. Barron, *Chem. Mater.* **2006**, *18*, 2602 – 2610.
[53] H.-X. Zhang, M. Kato, Y. Sasaki, T. Ohba, H. Ito, A. Kobayashi, H.-C. Chang, K. Uosaki, *Dalton Trans.* **2012**, *41*, 11497 – 11506.
[54] W. Lu, M. C. W. Chan, N. Zhu, C.-M. Che, C. Li, Z. Hui, *J. Am. Chem. Soc.* **2004**, *126*, 7639 – 7651.
[55] P. Xu, H. Wu, H. Jia, S. Ye, P. Du, *Organometallics* **2014**, *33*, 2738 – 2746.
[56] Z.-L. Gong, Y.-W. Zhong, J. Yao, *J. Mater. Chem. C* **2017**, *5*, 7222 – 7229.
[57] H. L. Au-Yeung, S. Y. Leung, V. W. Yam, *Chem. Commun.* **2018**, *54*, 4128 – 41331.
[58] B. Ma, P. I. Djurovich, S. Garon, B. Alleyne, M. E. Thompson, *Adv. Funct. Mater.* **2006**, *16*, 2438 – 2446.
[59] S. Sinn, F. Biedermann, L. De Cola, *Chem. Eur. J.* **2017**, *23*, 1965 – 1971.
[60] R. Soldati, A. Aliprandi, M. Mauro, L. De Cola, D. Giacomini, *Eur. J. Org. Chem.* **2014**, 7113 – 7121.
[61] D. Septiadi, A. Aliprandi, M. Mauro, L. De Cola, *RSC Adv.* **2014**, *4*, 25709 – 25718.
[62] M. Mydlak, M. Mauro, F. Polo, M. Felicetti, J. Leonhardt, G. Diener, L. De Cola, C. A. Strassert, *Chem. Mater.* **2011**, *23*, 3659 – 3667.

Manuscript received: March 29, 2020
Accepted manuscript online: April 23, 2020
Version of record online: July 1, 2020

